Initial Over-the-Air Performance Assessment of Ranging and Clock Synchronization Using Radio Frequency Signal Exchange

Patrick Bidigare, Scott Pruessing, David Raeman, Dzul Scherber
Raytheon BBN Technologies
Arlington, VA 22209
[pbidigare, spreussing, draeman, dscherber]@bbn.com

Upamanyu Madhow
ECE Department
University of California
Santa Barbara, CA 93106
madhow@ece.ucsb.edu

Raghu Mudumbai
ECE Department
The University of Iowa
Iowa City, IA 52242
rmudumbai@engineering.uiowa.edu

***Abstract*—In this paper we demonstrate results of a technique for synchronizing clocks and estimating ranges between a pair of RF transceivers. The technique uses a periodic exchange of ranging waveforms between two transceivers along with sophisticated delay estimation and tracking. The technique was implemented on wireless testbed transceivers with independent clocks and tested over-the-air in stationary and moving configurations. The technique achieved ~10ps synchronization accuracy and 2.1mm range deviation, using A two-channel oscilloscope and tape measure as truth sources. The timing resolution attained is three orders of magnitude better than the inverse signal bandwidth of the ranging waveform (50MHz => 6m resolution), and is within a small fraction of the carrier wavelength (915MHz => 327mm wavelength). We discuss how this result is consistent with the Weiss-Weinstein bound and cite new applications enabled by this technique.**

Keywords-Time Measurement; Wireless Networks; Filters; Tracking Loops; State Feedback

I. INTRODUCTION

In this paper we address the theory and implementation of a technique to enable network self-localization and clock synchronization across a wireless radio network. The technique readily generalizes to an N-node network, however the paper focuses on the two-node case. Our approach is to exchange waveforms between nodes in a line-of-sight propagation environment and exploit the reciprocity of propagation and anti-reciprocity of change-of-timebase to simultaneously estimate and track clock offset and propagation time. The technique is described in section II and the implementation of this technique on testbed radio platforms is discussed in section III. Over-the-air results are presented in section IV along with a comparison of our results with state-of-the-art GPS performance.

II. TECHNIQUE

A. Problem Formulation

Fig. 1 illustrates a two node network in which the offset between clocks and the RF propagation delay are treated as unknown stochastic processes. The nodes sequentially exchange RF ranging waveforms, recording and exchanging transmit and receive timestamps. These timestamps constitute measurements that can be used in a classical filtering framework [1] to estimate and track the unknown clock offsets and propagation delays.

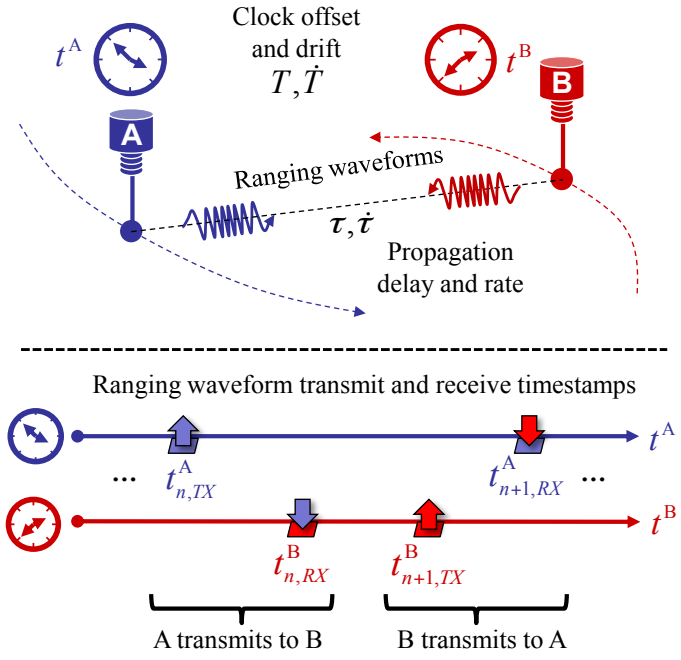

Fig. 1 Two-node ranging & synchronization technique.

B. State Space and Measurement Modeling

We define our state space to consist of the clock offset, clock drift, propagation delay and propagation delay rate:

$$\mathbf{x} := [T, \dot{T}, \tau, \dot{\tau}] \tag{1}$$

Two types of measurements take place. In the first, node A transmits a ranging waveform at time $t^A_{n,TX}$ (in A's timebase). The waveform is received by node B and a maximum

likelihood time-of-arrival (TOA) estimate $t^B_{n,RX}$ is constructed (in B's timebase). If we assume the clocks are running at nearly the same rate ($\dot{T} \approx 1$), and the range rate is much less than the speed of light ($\dot{\tau} \approx 0$), then the measurement equation is approximately given by

$$t^B_{n,RX} - t^A_{n,TX} \approx T_n + \tau_n + w_n, \tag{2}$$

where T_n, τ_n denote the offset and propagation delay at the time $t^A_{n,TX}$ the n^{th} ranging waveform is transmitted and w_n is the error (noise) in the receive-time measurement $t^B_{n,RX}$. The measurement equation for B transmitting to A (note reciprocal and anti-reciprocal terms) is

$$t^A_{n+1,RX} - t^B_{n+1,TX} \approx -T_{n+1} + \tau_{n+1} + w_{n+1}. \tag{3}$$

The time $t^B_{n+1,TX}$ of this measurement needs to be expressed in the A-timebase in which the filtering events are defined. Using the state space estimates we have

$$t^A_{n+1,TX} \approx \frac{t^B_{n+1,TX} - T_n + \dot{T}_n t^A_{n,TX}}{1 + \dot{T}_n}, \tag{4}$$

Our waveform receive times are obtained using the ML delay estimator technique described in [2]. In the high-SNR regime, this estimator allows unambiguous association of individual carrier cycles, achieving the timestamp estimates accurate to a small fraction of a carrier period, as promised by the Weiss-Weinstein bounds [3,4]. The variance of this ML estimator is asymptotically given by

$$E\left[|w_n|^2\right] = \frac{1}{8\pi^2 SNR\, f_c^2}. \tag{5}$$

where SNR is the integrated SNR and f_c is the center frequency of the transmission. The clock and propagation state parameters evolve according to

$$\begin{bmatrix} T_{n+1} \\ \dot{T}_{n+1} \end{bmatrix} = \begin{bmatrix} 1 & \Delta t_n \\ 0 & 1 \end{bmatrix} \begin{bmatrix} T_n \\ \dot{T}_n \end{bmatrix} + \begin{bmatrix} \nu_n^T \\ \nu_n^{\dot{T}} \end{bmatrix}, \tag{6}$$

$$\begin{bmatrix} \tau_{n+1} \\ \dot{\tau}_{n+1} \end{bmatrix} = \begin{bmatrix} 1 & \Delta t_n \\ 0 & 1 \end{bmatrix} \begin{bmatrix} \tau_n \\ \dot{\tau}_n \end{bmatrix} + \begin{bmatrix} \nu_n^\tau \\ \nu_n^{\dot{\tau}} \end{bmatrix}, \; \Delta t_n = t^A_{n+1,TX} - t^A_{n,TX}$$

The process noise covariance matrices have the form [1]

$$E\left[\begin{bmatrix} \nu_n^T \\ \nu_n^{\dot{T}} \end{bmatrix} \begin{bmatrix} \nu_n^T & \nu_n^{\dot{T}} \end{bmatrix}\right] = \underbrace{q_{11}^T \begin{bmatrix} \Delta t_n & 0 \\ 0 & 0 \end{bmatrix}}_{\text{White noise velocity}} + \underbrace{q_{22}^T \begin{bmatrix} \Delta t_n^3/3 & \Delta t_n^2/2 \\ \Delta t_n^2/2 & \Delta t_n \end{bmatrix}}_{\text{White noise acceleration}} \tag{7}$$

where the clock noise parameters q_{11}^T, q_{22}^T are chosen based on Allan deviation measurements of the clocks [5,6] and the kinematic noise parameters q_{11}^τ, q_{22}^τ can be chosen based on instrumented motion measurements.

The linearity of the measurement and evolution equations justifies the use of a Kalman filter for tracking the clock offset and propagation delay when the process and measurement noises are approximately Gaussian.

III. Implementation

A. Hardware

With careful attention to details, the technique is practical for implementation using off-the-shelf hardware components. A simplified block diagram of the hardware test platform built for over-the-air demonstration is presented in Fig. 2.

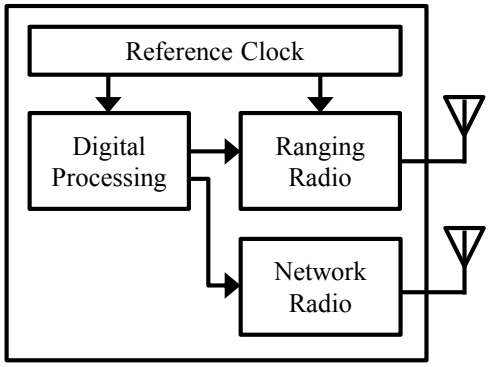

Fig. 2 Simplified block architecture of hardware.

The digital processing board contains a digital-to-analog converter (DAC), analog-to-digital converter (ADC), high-speed FPGA, and fixed-point digital signal processor. It performs TOA estimation and filter prediction, and it controls two radios.

The reference clock is an oven-controlled crystal oscillator (OCXO) [7] having an Allan deviation of less than 5 E-12 rms over a 1 second interval. It provides a common frequency-stable 10MHz reference for synthesizing the DAC and ADC clocks in the digital processing module and the carrier sinusoid in the ranging radio. These three clock domains must maintain a fixed phase relationship throughout operation and across power cycles.

The ranging radio uses a carrier frequency synthesizer that provides symmetric up and down conversion with a tunable center frequency between 200MHz and 2700MHz. It is used for exchanging ranging waveforms.

The network radio provides a channel between nodes to exchange timestamps. The hardware platform can operate using Ethernet, WiFi 802.11g, or an experimental long-range (2+ mile) ad-hoc networking radio.

B. Processing

After time slots are initially established, the ranging and time synchronization processing is performed cyclically on a scheduled basis.

1. At the start of a cycle, node B starts receiving on its ranging radio. Shortly after, node A transmits its ranging waveform.
2. Node A starts receiving on its ranging radio and node B transmits its ranging waveform.
3. Both nodes concurrently estimate time of arrival.
4. Timestamps are exchanged over the network radio.

5. Both nodes use these timestamps to update their Kalman filters.
6. The platform resources are now available for application-specific processing based on the configured re-estimation interval.
7. The estimated clock offset is used to maintain scheduled timeslot alignment in the common A-timebase.

To achieve absolute ranges and clock offsets, a hardware calibration procedure is required to account for node-specific group delays through the transmit and receive chains. This procedure has not yet been implemented, thus our estimation results currently apply only to changes in range and offset.

IV. Results

A. Experimental Setup

The ranging and synchronization technique was tested outdoors in a lightly wooded environment. Multiple sources of in-band interference were present. The system was tested in rain, fog and wind (clutter motion). The measured performance of the system includes all these effects.

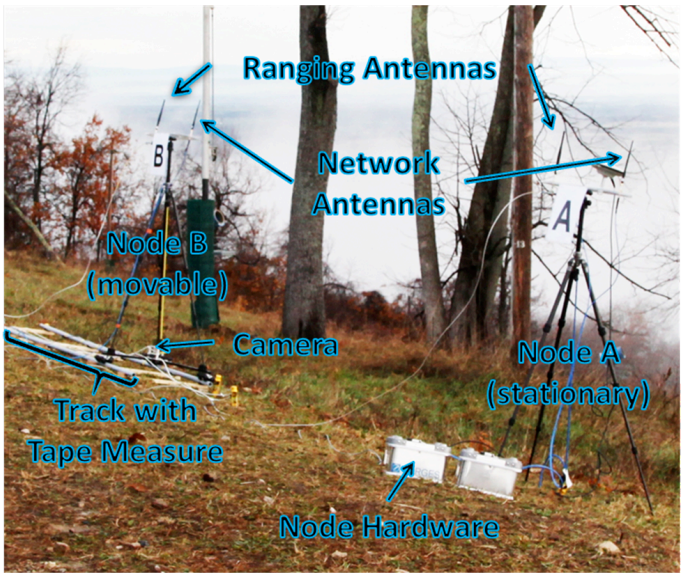

Fig. 3 Experimental setup of ranging and clock synchronization.

TABLE I. Experiment Parameters

Parameter	Value	Parameter	Value
Antenna height	2m	Center frequency	910MHz
Standoff	5.5m	Ranging WF bandwidth	50MHz
Transmit power	0.5W	Ranging WF duration	10us
Network radio	WiFi	Measurement frequency	10Hz

Fig. 3 shows the experimental setup. Two nodes were set up approximately 5.5 meters apart. Ranging and network antennas were mounted to tripods at fixed heights and orientations. A track formed by two PVC pipe struts anchored to the ground and a tripod platform mounted on caster wheels allowed node B to be moved linearly towards or away from node A. A measuring tape was secured to one of the struts and a digital video camera was mounted on the platform facing the tape. The tape/camera provided a source of truth for range changes.

B. Ranging Accuracy

A relative range standard deviation of $\sigma_{\text{range}} = 2.1\text{mm}$ was calculated using Kalman filter propagation time predictions obtained with the nodes in static positions:

$$\sigma_{\text{range}} = c\sqrt{\sum_{n=1}^{N}\left(T_n - \overline{T}\right)^2}, \quad \overline{T} = \sum_{n=1}^{N} T_n \tag{8}$$

Relative range estimation error was determined by fixing the position of node A's antenna and moving node B's antenna along the track. Fig. 4 shows the camera image of the tape measure and the Kalman filter estimate of the propagation time (converted to range). The range change closely tracked the truth with a slight negative bias that was smaller than the 2.1mm standard deviation.

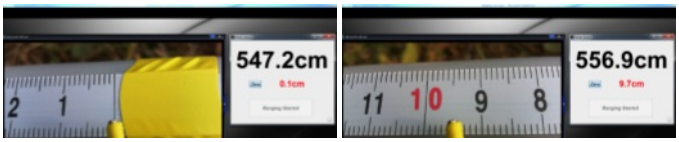

Starting Position Ending Position

Fig. 4 Screenshots of the system performance as a node moves along a track. The technique-measured change of means 556.75cm – 546.92 cm = 9.83cm closely matches the 9.5cm displacement seen on the tape measure.

C. Synchronization Accuracy

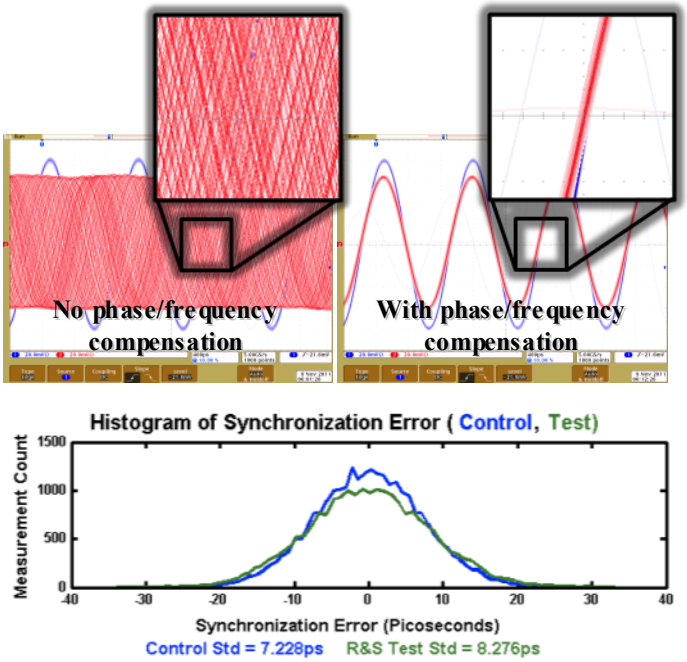

Fig. 5 Top: Oscilloscope traces of carriers (A and B) before and after synchronization. Total time extent: 4ns. Bottom: O-scope measurements of phase offset (R&S outdoor test vs. common source)

To verify synchronization and to measure error, we configured the nodes to digitally compensate their carrier phase and frequency based on the filter predictions. The antenna ports from transmitters A and B were split and connected to a two-channel oscilloscope that performed a phase comparison between the two signals. Figure 5 (green, bottom) shows a histogram of the synchronization error between the two nodes' carriers. A standard deviation of 8.3ps was measured using this method. Most of this error is due to limitations in the o-scope phase comparator, since the same two-channel measurement using a common 915MHz reference source yields a 7.2ps RMS error. If we assume clock synchronization to be independent of o-scope measurement error, then the effective synchronization error is $\sqrt{8.3^2 - 7.2^2} = 4$ps.

D. *Sources of Error*

In the real world environment in which this technique was tested, there were two sources of error present that were not part of our original model:

- Multipath: Significant RF scattering off the ground, nearby trees and poles contributed non-line of sight components to the received ranging waveform. These components tended to introduce a range-dependent bias in the measured timestamps.
- Non-stationary RF interference: Our time of arrival estimator implemented a prewhitening stage based on power spectral density (PSD) estimates of the interference collected during a quiescent training period. We noticed in-band interference sources that were time-slotted or otherwise non-stationary, which caused our PSD estimates to be stale when they were applied.

E. *Comparison with the State of the Art*

In order to compare our system's preliminary results with state of the art, we consider the synchronization and ranging accuracies associated with various uses of the line-of-sight signals from GPS satellites. The basic common comparison is the assumption of line-of-sight signal propagation.

Table II compares this performance with the state of the art; time synchronization on the left and ranging accuracy on the right. The synchronization approach in this paper demonstrates 500 times finer synchronization than Multi-channel GPS methods [8] and 10 times finer synchronization than carrier-phase based GPS [9]. These tests show ranging accuracies more than 1000 times finer than WAAS GPS [10] and nearly a four times finer than real-time kinematic GPS [11].

TABLE II. COMPARISON OF RANGING AND SYNCHRONIZATION PERFORMANCE AGAINST COMMERCIAL STATE-OF-THE-ART

Sync Method	**Accuracy**	**Ranging Method**	**Accuracy**
Multi-Channel GPS	5000 ps	GPS w/ WAAS	2.4 m
Carrier Phase GPS	100 ps	RTK GPS	11 mm
Ranging and Synchronization	<10 ps	Ranging and Synchronization	2.1 mm

V. CONCLUSIONS

The technique developed in this paper allows the clock offset and range between a pair of radio nodes to be estimated and tracked. We implemented this technique in embedded software and firmware running on an experimental off-the-shelf hardware platform. Over-the-air testing demonstrated propagation and clock offset estimation errors far smaller than either the temporal resolution or the carrier period of the ranging waveform. The demonstrated performance is significantly better than the most advanced commercial techniques for clock synchronization or range estimation. This degree of synchronization and ranging accuracy makes possible distributed communications and sensing techniques that require coherence across a wireless ad-hoc network of radios.

In the future, we hope to extend this work by:

- Implementing a hardware calibration procedure to allow absolute range measurements to be obtained.
- Enhancing the TOA estimation technique to be robust in strong multipath scattering environments.
- Generalizing the 2-node range estimation to a general N-node network self-localization technique in which the (x, y, z) positions of all nodes are tracked in a node-centric coordinate system.

REFERENCES

[1] Y. Bar-Shalom, X.R. Li, T. Kirubarajan, "Estimation with applications to tracking and navigation," John Wiley & Sons, Inc., 2001.

[2] P. Bidigare, U. Madhow, R. Mudumbai, D. Scherber, "Attaining fundamental bounds on timing synchronization," IEEE International Conference on Acoustics, Speech and Signal Processing, (ICASSP), in press, Mar. 2012.

[3] A. Weiss and E. Weinstein, "Fundamental limitations in passive time delay estimation-part i: Narrow-band systems," Acoustics, Speech and Signal Processing, IEEE Transactions on, vol. 31, no. 2, pp.472-286, Apr 1983.

[4] E. Weinstein and A. Weiss, "Fundamental limitations in passive time-delay estimation-part ii: Wide-band systems,"Acoustics, Speech and Signal Processing, IEEE Transactions on, vol. 32, no. 5, pp.1064-1078, Oct 1984.

[5] C. Zucca and P. Tavella, "The clock model and its relationship with the allan and related variances," Ultrasonics, Feroelectrics and Frequency Control, IEEE Transactions on, vol. 52, pp.289-296, Feb. 2005.

[6] Lorenzo Galleani, "A tutorial on the two-state model of the atomic clock noise," Metrologia, vol. 45, no. 6 pp.S175-S182, Dec. 2008.

[7] Rakon, "Crystal Oscillator Specification CFPO DO-1 @ 10MHz," Oct. 2010.

[8] M.A. Lombardi, L.M. Nelson, A.N. Novick, V.S. Zhang, "Time and frequency measurements using the global positioning system," Cal. Lab. Int. Jour. Of Metrology, Jul-Sept 2001, pp. 26-33.

[9] K.M. Larson, J. Levine, "Carrier-phase time transfer," Ultrasonics, Ferroelectrics, and Frequency Control, IEEE Transactions on, vol.46, no. 4, Jul. 1999.

[10] NSTB/WAAS T&E Team, "Wide-area augmentation system performance analysis report: report #39", FAA/William J. Hughes Technical Center, Jan. 2012.

[11] NovAtel, "AdVance RTK competative analysis," Version 2-013882 Specifications, Apr. 2011 [Online]. Available: http://novatel.com/Documents/Papers/AdVanceRTK.pdf. [Accessed Feb. 2012]